JACS
JOURNAL OF THE AMERICAN CHEMICAL SOCIETY

COMMUNICATION

pubs.acs.org/JACS

Facile Synthesis of Silver Chalcogenide (Ag_2E; E = Se, S, Te) Semiconductor Nanocrystals

Ayaskanta Sahu,[†] Lejun Qi, Moon Sung Kang, Donna Deng, and David J. Norris*[,†]

Department of Chemical Engineering and Materials Science, University of Minnesota, 421 Washington Avenue SE, Minneapolis, Minnesota 55455, United States

Supporting Information

ABSTRACT: A general, one-pot, single-step method for producing colloidal silver chalcogenide (Ag_2E; E = Se, S, Te) nanocrystals is presented, with an emphasis on Ag_2Se. The method avoids exotic chemicals, high temperatures, and high pressures and requires only a few minutes of reaction time. While Ag_2S and Ag_2Te are formed in their low-temperature monoclinic phases, Ag_2Se is obtained in a metastable tetragonal phase not observed in the bulk.

As a bulk material, silver selenide (Ag_2Se) is a narrow-band-gap semiconductor with many intriguing properties. First, it is a mixed conductor with high electronic and ionic mobility. Second, it undergoes a reversible first-order phase transition from a low-temperature phase (α-Ag_2Se) to a high-temperature phase (β-Ag_2Se) at 135 °C with a strong change in its electronic properties.[1] β-Ag_2Se is a superionic conductor that is used as an additive in highly conductive composite glasses for sensors, displays, and photochargeable secondary batteries and has potential as a solid electrolyte.[2] α-Ag_2Se is widely used as a thermoelectric material because of its high electrical conductivity, large Seebeck coefficient, and low thermal conductivity and as a photosensitizer in photographic films and thermochromic materials.[3] Nonstoichiometric α-$Ag_{2+\delta}Se$ also shows giant magnetoresistance comparable to the colossal magnetoresistance observed in manganese perovskites.[4,5]

However, while all of these properties have been studied extensively in the bulk, very few reports have examined nanoscale Ag_2Se. In many semiconductors, decreasing the size of the material can provide a way to tune the physical properties and observe new phenomena. In particular, colloidal semiconductor nanocrystals provide strongly size-specific optical and optoelectronic properties. These have been investigated for potential applications in solar cells,[6] light-emitting diodes,[7,8] thin-film transistors,[9,10] and biological imaging.[11,12] Therefore, if uniformly sized Ag_2Se nanocrystals were available, they could provide an interesting new system for investigation of the dependence of optical, magnetic, mechanical, and transport properties on size. Furthermore, high-quality Ag_2Se nanocrystals could lead to new applications or could significantly improve the performance of existing applications. These factors provide a compelling motivation to synthesize and explore the properties of Ag_2Se nanocrystals and extend the versatility of these materials simply by tailoring parameters such as size, stoichiometry, or crystal phase.

Despite this motivation, the synthesis of high-quality Ag_2Se semiconductor nanocrystals is much less developed than those of other materials such as the cadmium and zinc chalcogenides. Of the silver chalcogenides, Ag_2S has been the most studied.[13−17] Only a few reports on the preparation of Ag_2Se nanoparticles,[18,19] nanowires,[20] and nanoscale dendrites[21] exist. Other routes for obtaining nanosized Ag_2Se include vapor-phase growth,[22] sonochemical methods,[23] and high-temperature[22] and high-pressure[24] solution-phase reactions. These methods often require the use of exotic precursors[25] and extreme conditions. Nevertheless, they still generate Ag_2Se nanocrystals that are polycrystalline and polydisperse, which can severely limit their use in both fundamental studies and potential applications.

To obtain crystalline, nearly monodisperse Ag_2Se particles, one could adapt a successful recipe for Ag_2Te nanocrystals.[26] Unfortunately, this synthesis requires 2 weeks. Alternatively, one could perform cation exchange on CdSe nanocrystals or transform Ag nanocrystals to Ag_2Se.[18,19] However, this involves a two-step process involving the synthesis of either CdSe or Ag nanocrystals followed by the transformation. Therefore, to the best of our knowledge, no reported method is direct, simple, and fast.

Here we demonstrate a one-pot, single-step synthesis of structurally well-defined and nearly monodisperse Ag_2Se nanocrystals. Our route is advantageous because it utilizes low temperature, atmospheric pressure, and standard chemicals. Instead of days, the reaction is complete within a few minutes. Moreover, the method also works for the synthesis of Ag_2S and Ag_2Te nanocrystals, thus providing a general and versatile technique to obtain the entire family of silver chalcogenides.

In a typical synthesis, 16.99 g of $AgNO_3$ and 7.896 g of selenium shot were dissolved separately in 100 mL tri-*n*-octylphosphine (TOP) to obtain 1 M Ag−TOP and 1 M TOP−Se, respectively. A mixture of 6.4 mL of oleic acid (OA), 5.4 g of 1-octadecylamine (ODA), and 12.8 mL of 1-octadecene (ODE) was then combined in a 100 mL round-bottom flask, degassed, flushed three times with N_2 to remove water and oxygen, and heated to 70 °C under N_2. With continuous stirring, 4 mL of TOP−Se was added into the flask, and the temperature was raised to 160 °C. Next, 4 mL of Ag−TOP was quickly injected, and the reaction was allowed to proceed for ∼5 min at 150 °C. The growth was quenched in an ice bath, and 25 mL of butanol was added to prevent solidification of the reaction mixture as it cooled. The nanocrystals were isolated by precipitation with ethanol and redispersed in hexanes. This process was repeated at

Received: January 1, 2011
Published: April 12, 2011

dx.doi.org/10.1021/ja200012e | J. Am. Chem. Soc. 2011, 133, 6509–6512

least once to ensure a clean product. Similar syntheses were developed to obtain Ag_2S and Ag_2Te nanocrystals. For all three, we could also obtain nanocrystals with different average sizes by varying the reaction time and growth temperature. The as-obtained nanocrystals can be dispersed in various organic solvents, such as hexanes, toluene, or chloroform. Further synthetic details are given in the Supporting Information (SI).

In general, Ag_2E nanocrystals can plate a glass container with silver if stored under ambient conditions. When they were dispersed in hexanes, this effect occurred for our Ag_2Se and Ag_2Te nanocrystals after ca. 4 and 3 weeks, respectively. However, under storage at −20 °C in the dark, these nanocrystals have remained stable indefinitely (for 8 and 4 months, respectively, as of this writing). Our Ag_2S nanocrystals have been stable for 7 months even under ambient conditions. For all of the samples, the stability decreased when excess surface ligands were removed from the dispersion by repeated precipitations. Use of solvents other than hexanes also reduced the stability (see the SI for details).

Transmission electron microscopy (TEM) images of a typical Ag_2Se sample are shown in Figure 1a,b. The nanocrystals are nearly monodisperse with a standard deviation of 5.1% and an average size of ca. 6.5 nm. This value is consistent with the average size of the crystallographic domains calculated by fitting the X-ray diffraction (XRD) patterns (discussed below) using the Scherrer equation. A representative high-resolution TEM (HRTEM) image of the Ag_2Se nanocrystals demonstrates that they are single-crystalline (Figure 1b). Characteristic TEM images of Ag_2S (Figure 1d,e) and Ag_2Te (Figure 1g,h) nanocrystals are also shown. The standard deviations in size were 5.3 and 9.1% for Ag_2S and Ag_2Te, respectively. The samples exhibited sensitivity to the electron beam, as discussed in the SI. This affected the quality of the HRTEM images.

To clarify the sample composition and verify that both elements were present in the nanocrystals, several spectroscopic techniques were employed. Figure 2a−c presents X-ray photoelectron spectroscopy (XPS) data for the Ag_2Se nanocrystals (see the SI for Ag_2Te and Ag_2S data). The survey spectrum combined with the core-level spectra, which clearly show Ag 3d and Se 3p peaks, indicate that Ag and Se were present. Quantitative determination of the chemical composition was performed with electron-probe microanalysis (EPMA). This showed that the Ag:E elemental ratios for E = Se, Te, and S were 1.85:1 (±1.7%), 2.14:1 (±6.7%), and 1.94:1 (±1.5%), respectively (see the SI), all of which are close to the expected ratio of 2:1.

All three silver chalcogenides were also expected to exhibit temperature-dependent polymorphism. In our syntheses, even though the growth temperatures of Ag_2Se and Ag_2Te were above their respective $\alpha \rightarrow \beta$ phase-transition temperatures (135 and 150 °C,[27] respectively), selected-area electron diffraction (SAED) patterns (Figure 1c,f,i) and powder XRD patterns of the particles' crystallographic structure (Figure 3a) revealed that none of the final products were in their high-temperature phases. For Ag_2S and Ag_2Te, the equilibrium low-temperature phases, namely, α-Ag_2S (monoclinic, JCPDS no. 00-014-0072) and α-Ag_2Te (monoclinic, JCPDS no. 00-034-0142), were observed. For Ag_2Se, it has previously been postulated that two low-temperature phases (stable orthorhombic and metastable tetragonal) exist, depending on the crystallite size.[28,29] Although XRD patterns for the tetragonal phase of Ag_2Se were not available in the database, a careful analysis of our data indicated that all of our Ag_2Se nanocrystals were in the metastable tetragonal phase

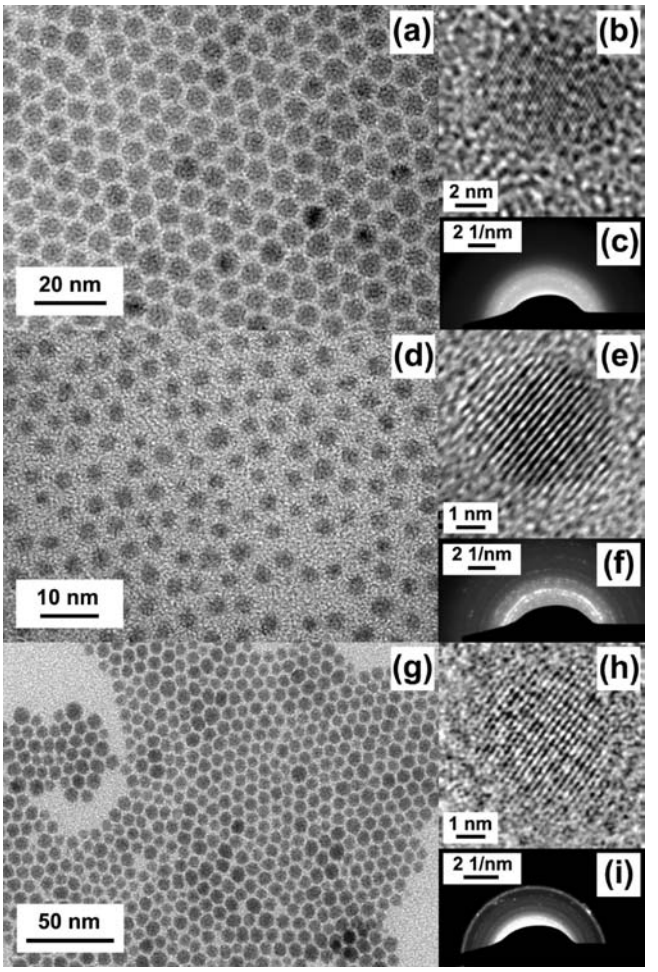

Figure 1. Low-magnification TEM micrographs and SAED patterns of ensembles of as-synthesized nanocrystals of (a, c) Ag_2Se, (d, f) Ag_2S, and (g, i) Ag_2Te along with lattice-resolved HRTEM micrographs of single (b) 7 nm diameter Ag_2Se, (e) 4 nm diameter Ag_2S, and (h) 7 nm diameter Ag_2Te nanocrystals. Injection temperatures of 197 and 191 °C and growth times of 12 min at ∼167 °C and 5 min at ∼150 °C were used to produce the Ag_2S and Ag_2Te nanocrystals, respectively.

(having lattice constants $a = b = 0.706$ nm and $c = 0.498$ nm) instead of the more stable orthorhombic phase (details can be found in the SI). These results suggest that (i) Ag_2Se and Ag_2Te nanocrystals undergo first-order phase transitions to a low-temperature phase upon cooling from the reaction temperature and (ii) Ag_2Se nanocrystals are kinetically trapped in a metastable phase that is not observed in the bulk. TEM and XRD studies with in situ heating are underway to test these two conclusions.

We also note that similar XRD patterns for Ag_2Se nanocrystals have previously been assigned to other crystal structures. On the basis of our analysis, we believe the prior assignment to the orthorhombic phase is incorrect.[18] Also, small Ag_2Se nanocrystals (ca. 4 nm in size) had been assigned to the cubic phase.[19] Our smallest nanocrystals (ca. 3 nm in size) did indeed exhibit an XRD pattern that could be attributed to the cubic phase. However, the most prominent XRD peaks for the tetragonal and cubic phases overlap. Thus, as a result of Scherrer broadening, these two phases are difficult to distinguish in small nanocrystals. Because our larger Ag_2Se nanocrystals were clearly

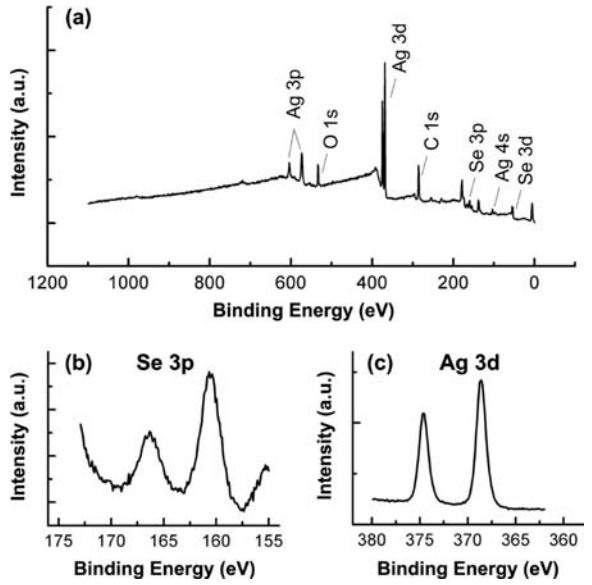

Figure 2. (a) XPS survey spectrum of Ag_2Se nanocrystals showing the presence of both Ag and Se. (b, c) High-resolution XPS spectra of Ag_2Se from (b) Se 3p and (c) Ag 3d.

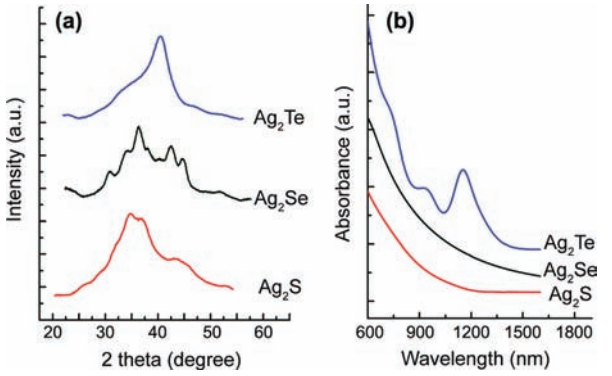

Figure 3. (a) XRD patterns and (b) room-temperature optical absorbance spectra of as-synthesized Ag_2Te, Ag_2Se, and Ag_2S nanocrystals. The observed peak broadening in the reflections due to size is expected.

in the tetragonal phase (see the SI), we believe it is more likely that all of our sizes had the tetragonal structure. This conclusion also agrees with other reports.[28,29] This implies that all of our Ag_2Se nanocrystals were trapped in a metastable crystal structure.

We also need to address the role of ODE, TOP, OA, and ODA in the nanocrystal growth. Our evidence suggests that ODE acts simply as a noncoordinating solvent. While TOP, OA, and ODA can all potentially act as surface ligands that stabilize the nanocrystals and mediate the growth, Fourier-transform IR (FTIR) measurements (see the SI) showed that the surfaces of the Ag_2Se and Ag_2Te nanocrystals were covered almost entirely with TOP. This is consistent with the precursors for these materials (Ag−TOP, TOP−Se, and TOP−Te). For Ag_2S, where sulfur powder was first dissolved in ODA and OA, these ligands were also detected on the nanocrystal surface, but only weakly. We believe instead that ODA and OA are important for controlling the reaction rate. Without ODA, large precipitates of Ag_2Te and Ag_2Se formed in seconds and minutes, respectively. (With Ag_2S, large but stable 10−12 nm nanocrystals were obtained.) Without OA, the growth proceeded extremely slowly, yielding small, polydisperse nanocrystals. Thus, by balancing these two effects, a mixture of OA and ODA produced nearly monodisperse samples.

The optical absorption spectra of dispersions in tetrachloroethylene are shown in Figure 3b. The Ag_2Te spectrum shows three clearly resolved transitions, as observed previously.[26,30] Surprisingly, the spectra from our Ag_2S and Ag_2Se samples are featureless, even though the nanocrystals had much narrower size distributions (∼5%) than our Ag_2Te sample (∼9%). We also found that the Ag_2Te absorption features are not size-dependent, at least over the size range accessible to us (ca. 3−8 nm in diameter). The explanation for these transitions and the absence of similar features in our Ag_2Se and Ag_2S nanocrystals is still under investigation.

In conclusion, a simple route to nearly monodisperse colloidal Ag_2Se nanocrystals has been presented. This synthesis can also be adapted to yield Ag_2S and Ag_2Te nanocrystals. The particles are nearly stoichiometric and single-crystalline. Ag_2S and Ag_2Te are produced in their low-temperature equilibrium phases. For Ag_2Se, the metastable tetragonal phase is obtained. Because of the simplicity and adaptability of the synthesis in terms of size and materials, a variety of new nanoscale silver chalcogenides can be obtained. These materials have unique properties, and the nanocrystals should allow new phenomena and applications to be explored.

■ ASSOCIATED CONTENT

Ⓢ Supporting Information. Details of the syntheses of Ag_2S and Ag_2Te nanocrystals, EPMA measurements, FTIR spectra, and XPS and XRD data and analysis. This material is available free of charge via the Internet at http://pubs.acs.org.

■ AUTHOR INFORMATION

Corresponding Author
dnorris@ethz.ch

Present Addresses
[†]Optical Materials Engineering Laboratory, ETH Zurich, Universitätstrasse 6, 8092 Zürich, Switzerland.

■ ACKNOWLEDGMENT

The authors thank Ellery Frahm for help with EPMA measurements and Jeffrey Urban and Dong Kyun Ko for valuable suggestions. This work was primarily supported by the National Science Foundation (NSF) Materials World Network under DMR-0908629. Additional support was provided by the Industrial Partnership for Research in Interfacial and Materials Engineering (IPRIME) at the University of Minnesota (UMN). This work also utilized the Characterization Facility at UMN, which has received support from the NSF through the MRSEC, NNIN, ERC, and MRI Programs.

■ REFERENCES

(1) Schoen, D. T.; Xie, C.; Cui, Y. *J. Am. Chem. Soc.* **2007**, *129*, 4116–4117.
(2) Boolchand, P.; Bresser, W. J. *Nature* **2001**, *410*, 1070–1073.
(3) Ferhat, M.; Nagao, J. *J. Appl. Phys.* **2000**, *88*, 813–816.

(4) Parish, M. M.; Littlewood, P. B. *Nature* **2003**, *426*, 162–165.
(5) Xu, R.; Husmann, A.; Rosenbaum, T. F.; Saboungi, M. L.; Enderby, J. E.; Littlewood, P. B. *Nature* **1997**, *390*, 57–60.
(6) Gur, I.; Fromer, N. A.; Geier, M. L.; Alivisatos, A. P. *Science* **2005**, *310*, 462–465.
(7) Colvin, V. L.; Schlamp, M. C.; Alivisatos, A. P. *Nature* **1994**, *370*, 354–357.
(8) Tessler, N.; Medvedev, V.; Kazes, M.; Kan, S.; Banin, U. *Science* **2002**, *295*, 1506–1508.
(9) Klein, D. L.; Roth, R.; Lim, A. K. L.; Alivisatos, A. P.; McEuen, P. L. *Nature* **1997**, *389*, 699–701.
(10) Talapin, D. V.; Murray, C. B. *Science* **2005**, *310*, 86–89.
(11) Chan, W. C. W.; Nie, S. *Science* **1998**, *281*, 2016–2018.
(12) Bruchez, M., Jr.; Moronne, M.; Gin, P.; Weiss, S.; Alivisatos, A. P. *Science* **1998**, *281*, 2013–2016.
(13) Hoyer, P.; Weller, H. *Chem. Phys. Lett.* **1994**, *224*, 75–80.
(14) Motte, L.; Billoudet, F.; Lacaze, E.; Douin, J.; Pileni, M. P. *J. Phys. Chem. B* **1997**, *101*, 138–144.
(15) Gao, F.; Lu, Q.; Zhao, D. *Nano Lett.* **2003**, *3*, 85–88.
(16) Huxter, V. M.; Mirkovic, T.; Nair, P. S.; Scholes, G. D. *Adv. Mater.* **2008**, *20*, 2439–2443.
(17) Du, Y.; Xu, B.; Fu, T.; Cai, M.; Li, F.; Zhang, Y.; Wang, Q. *J. Am. Chem. Soc.* **2010**, *132*, 1470–1471.
(18) Wang, D.; Xie, T.; Peng, Q.; Li, Y. *J. Am. Chem. Soc.* **2008**, *130*, 4016–4022.
(19) Son, D. H.; Hughes, S. M.; Yin, Y.; Alivisatos, A. P. *Science* **2004**, *306*, 1009–1012.
(20) Gates, B.; Wu, Y.; Yin, Y.; Yang, P.; Xia, Y. *J. Am. Chem. Soc.* **2001**, *123*, 11500–11501.
(21) Xiao, J.; Xie, Y.; Tang, R.; Luo, W. *J. Mater. Chem.* **2002**, *12*, 1148–1151.
(22) Safran, G.; Geszti, O.; Radnoczi, G.; Barna, P. B. *Thin Solid Films* **1998**, *317*, 72–76.
(23) Wang, W. Z.; Geng, Y.; Qian, Y. T.; Ji, M. R.; Xie, Y. *Mater. Res. Bull.* **1999**, *34*, 877–882.
(24) Henshaw, G.; Parkin, I. P.; Shaw, G. A. *J. Chem. Soc., Dalton Trans.* **1997**, 231–236.
(25) Ng, M. T.; Boothroyd, C.; Vittal, J. J. *Chem. Commun.* **2005**, 3820–3822.
(26) Urban, J. J.; Talapin, D. V.; Shevchenko, E. V.; Kagan, C. R.; Murray, C. B. *Nat. Mater.* **2007**, *6*, 115–121.
(27) Qin, A. M.; Fang, Y. P.; Tao, P. F.; Zhang, J. Y.; Su, C. Y. *Inorg. Chem.* **2007**, *46*, 7403–7409 .
(28) Gunter, J. R.; Keusch, P. *Ultramicroscopy* **1993**, *49*, 293–307.
(29) Gates, B.; Mayers, B.; Wu, Y. Y.; Sun, Y. G.; Cattle, B.; Yang, P. D.; Xia, Y. N. *Adv. Funct. Mater.* **2002**, *12*, 679–686.
(30) Ko, D.-K.; Urban, J. J.; Murray, C. B. *Nano Lett.* **2010**, *10*, 1842–1847.